



Seasonal dependence and solar wind control of transpolar arc luminosity

A. Kullen,¹ J. A. Cumnock,^{2,3} and T. Karlsson²

Received 9 February 2008; revised 9 February 2008; accepted 13 March 2008; published 27 August 2008.

[1] The influence of the solar wind and the interplanetary magnetic field (IMF) on the luminosity of transpolar arcs (TPAs) is examined by taking into account seasonal effects. The study focuses on those transpolar arcs that appear after an IMF B_y sign change during steady northward IMF. It includes 21 northern hemisphere events identified in a previous study from global UV images taken by the Polar spacecraft between 1996 and 2000. Sorting the TPA events by sign of the Earth dipole tilt we find that the TPAs which appear in the dark hemisphere are on average much weaker than TPAs in the sunlit hemisphere. For the dark hemisphere events, no clear correlation between solar wind parameters and TPA luminosity is found. However, in the sunlit hemisphere, a clear dependence on solar wind and IMF conditions is seen. The TPA brightness is strongly influenced by IMF magnitude, northward IMF B_z and solar wind speed. A weak, negative correlation with the ion density is found. The TPA luminosity in the sunlit hemisphere is much more strongly controlled by the magnetic energy flux than by the kinetic energy flux of the solar wind. This explains the absence of transpolar arcs for the two B_y sign change cases for positive dipole tilts with lowest magnetic energy flux values. The strong influence of the Earth dipole tilt on the transpolar arc luminosity appears due to the dependence of the ionospheric conductivity on solar EUV emissions.

Citation: Kullen, A., J. A. Cumnock, and T. Karlsson (2008), Seasonal dependence and solar wind control of transpolar arc luminosity, *J. Geophys. Res.*, 113, A08316, doi:10.1029/2008JA013086.

1. Introduction

1.1. Solar Wind Influence on Auroral Luminosity

[2] It is generally understood that the auroral pattern and the auroral activity are strongly influenced by the solar wind and the interplanetary magnetic field (IMF). The strongest correlation between auroral luminosity and solar wind parameters is found for the IMF B_z component. *Liou et al.* [1998] observed a linear dependence between southward IMF and mean auroral power (derived from the auroral luminosity measurements by the Polar UV imager). The dependence on northward IMF is more complicated. In the afternoon sector the auroral power increases slowly with increasing positive IMF B_z . At the nightside oval the auroral power is generally very low during northward IMF.

[3] Solar wind velocity and density influence the auroral brightness as well. Looking at the solar wind velocity effect on the auroral brightness statistically, a positive correlation was found [*Liou et al.*, 1998; *Shue et al.*, 2002]. The statistical dependence on the solar wind density is less clear. *Liou et al.* [1998] found no clear correlation for the

afternoon and a negative correlation at the nightside oval. However, *Shue et al.* [2002] reported a positive density correlation in the nightside oval section. Many authors have reported that sudden pressure pulses cause the aurora to brighten [e.g., *Elphinstone et al.*, 1991; *Zhou and Tsurutani*, 1999; *Liou et al.*, 2002]. *Liou et al.* [2005] showed that a solar wind pressure pulse can even cause auroral enhancements along a transpolar arc.

[4] In some statistical auroral luminosity studies, the polar cap area is shown as well. *Baker et al.* [2003] examined the dependence of the auroral luminosity on interplanetary parameters during one winter month. From their figures it can be seen that the average auroral luminosity in the polar cap has a similar dependence on IMF and solar wind as the aurora in the main oval, away from the nightside sector. Polar cap aurora is shown to correlate well with northward IMF and solar wind speed. A weak, negative correlation is seen for the solar wind density and IMF B_x . Although not explicitly addressed by *Shue et al.* [2002], their figures indicate a negative dependence of polar cap aurora on the solar wind density during the summer.

[5] Generally the dependence of the auroral brightness on solar wind density, velocity and season are much more pronounced during southward than during northward IMF [*Shue et al.*, 2002]. This difference can be explained by a much more efficient energy coupling between the solar wind and the magnetosphere for southward IMF due to a more favorable magnetic topology that allows magnetic reconnection along the dayside magnetopause [*Dungey*, 1961]. During northward

¹Swedish Institute of Space Physics, Uppsala, Sweden.

²Space and Plasma Physics, School of Electrical Engineering, Royal Institute of Technology, Stockholm, Sweden.

³Also at Center for Space Sciences, University of Texas at Dallas, Richardson, Texas, USA.

IMF the energy transfer takes place through high-latitude lobe reconnection [e.g., *Kessel et al.*, 1996 and references therein]. While the IMF B_z component determines the location and efficiency of the reconnection site, the magnetic solar wind energy flux determines the amount of energy that enters the magnetosphere [*Akasofu*, 1980].

1.2. Seasonal Dependence of Auroral Luminosity

[6] The effect of solar wind parameters on the auroral luminosity is diluted by the strong influence of sunlight on the ionosphere. The auroral brightness varies considerably with season. The EUV illumination ionizes the upper part of the atmosphere, leading to a higher conductivity in sunlit regions, and thus enhances the production rate of aurora.

[7] For the duskside and dayside oval this is confirmed by several studies. Although the polar cap is not addressed explicitly by *Shue et al.* [2001b], it is clearly seen that the average auroral luminosity of the polar cap has a similar dependence on season as does the dayside oval. However, on the nightside the opposite dependence on season is observed: *Liou et al.* [2001] and *Shue et al.* [2001b] used Polar UVI images to study seasonal effects on the auroral brightness. They both found that dayside aurora is slightly brighter during summer, while the nightside aurora is much brighter during the winter.

[8] According to *Shue et al.* [2001a] the different seasonal dependencies of day- and nightside aurora are connected to the difference between diffuse aurora and discrete arcs. The summer enhancement of the mainly diffuse dayside aurora is explained in *Shue et al.* [2001a] and *Ohtani et al.* [2005] by the linear dependence of the dayside FACs on the ionospheric conductivity, that has been observed by *Fujii and Iijima* [1987]. The conductance is sufficient to satisfy the FAC requirement, and no field-parallel E-fields are necessary to maintain the current balance, thus, no discrete arcs appear. As suggested by *Fujii and Iijima* [1987] this indicates a voltage generator in the plasma sheet.

[9] The suppression of discrete arcs in sunlight has first been reported by *Newell et al.* [1996]. From the statistical distribution of accelerated electron events *Newell et al.* [1996] concluded that most discrete arcs are concentrated in the dusk-nightside sector of the oval. They suggested that the high occurrence frequency of discrete arcs in this region has to do with an originally extremely low conductivity due to a lack of particles. The low density in the premidnight region appears because the hot electrons from the Earth's plasma sheet map to the dawnside oval due to curvature and gradient drifts, leading to a broad region of mainly diffuse aurora with moderately high conductivity at the dawn oval. To maintain a current system between the magnetosphere and a low conductivity region, electrons become accelerated and establish a higher conductivity, as the electron precipitation ionizes the upper ionosphere. This so-called feedback mechanism (first introduced by *Atkinson* [1970]) can only take place in a region of upward FACs with a low background conductivity, such as the premidnight oval sector.

1.3. Solar Wind Influence on the Occurrence Frequency of Polar Arcs

[10] The polar cap region is often neglected due to its lack of precipitating particles during geomagnetic active times

when the IMF is southward. The quiet state of the magnetosphere prevails for B_z near zero, while for northward IMF the polar cap becomes active [*Gussenhoven*, 1988]. During northward IMF conditions, field-aligned currents (NBZ currents) can be measured inside the polar cap [*Iijima et al.*, 1984], and small-scale sun-aligned arcs appear frequently [*Valladares et al.*, 1994]. Also large-scale polar arcs are a predominately northward phenomenon [*Kullen et al.*, 2002]. The evolution of polar arcs is strongly controlled by the direction of the IMF. *Valladares et al.* [1994] showed that small-scale polar arcs appear mainly during northward IMF and negative B_x . Their location and motion depends on IMF B_y , *Kullen et al.* [2002] found a similar relation for large-scale polar arcs. Dependent on the IMF clock angle, different types of polar arcs develop. Those polar arc types that reach a considerably poleward location (denoted in *Kullen et al.* [2002] as midnight, moving and multiple arcs) appear predominantly during positive IMF B_z , negative IMF B_x , high IMF magnitude and solar wind velocity. No dependence on solar wind density or pressure was found.

[11] Both, an IMF B_z turn to southward IMF [*Newell and Meng*, 1995] and an IMF B_y sign change during northward IMF [*Cumnock et al.*, 1997] can trigger large-scale polar arcs to move to highest latitudes. When the IMF turns southward during positive (negative) IMF B_y , an arc starts to bend from the dawn (dusk) oval side into the polar cap (*Kullen et al.* [2002], described as the "bending arc" type). A change from positive to negative (negative to positive) IMF B_y causes a rather sun-aligned arc to separate from the dusk (dawn) oval side and to move over the entire polar cap (*Cumnock et al.* [1997]; for nice examples see also *Cumnock et al.* [2002]). While *Kullen et al.* [2002] called this type of arc "moving arc", most authors use the expression "theta aurora" or "transpolar arc", which is, strictly speaking, only true during the time the arc appears in the middle of the polar cap. In this study, we will use the more common description "transpolar arc" (TPA) to describe polar auroral arcs triggered by an IMF B_y sign change.

[12] During many events the IMF is highly varying, and both IMF B_y and B_z sign changes influence the evolution of a TPA simultaneously (see e.g., the events presented by *Chang et al.* [1998]). This has caused a lot of confusion in the research community regarding the relative importance of the different IMF changes. To clarify the role of IMF B_y , *Cumnock* [2005] made a large survey through several years of solar wind data to identify all time periods with a single IMF B_y sign change during several hours of steady northward IMF for which global auroral images from Polar UVI were available. They were able to detect transpolar arcs in nearly all cases, which shows that an IMF B_y sign change during northward IMF is indeed sufficient to trigger a TPA.

1.4. Seasonal and Solar Wind Dependence of Polar Arc Luminosity

[13] The seasonal dependence of single auroral arcs appearing poleward of the main oval has been addressed by *Frey et al.* [2004] for localized high-latitude dayside aurora (HiLDA) and by *Cumnock* [2005] for TPAs. *Frey et al.* [2004] observed a maximum occurrence of HiLDAs during sunlit summer months and an almost complete absence in the dark winter. *Cumnock* [2005] found a similar seasonal dependence of the TPA luminosity. On average,

summer TPAs are much brighter than winter arcs. However, they did not find any clear connection between solar wind parameters and the auroral luminosity of TPAs.

[14] In this study, we continue the work of *Cumnock* [2005]. We investigate a possible solar wind dependence of the TPA luminosity by sorting the events into sunlit (positive Earth dipole tilt) and dark hemisphere events (negative Earth dipole tilt) to take seasonal effects into account.

2. Observations

[15] This work is based on a slightly extended list of northern hemisphere TPAs by *Cumnock* [2005]. The TPAs are identified and their luminosity determined with help of global auroral images from the UV imager on the Polar spacecraft (Polar UVI), the solar wind conditions are analyzed using the OMNIWeb data set.

[16] *Cumnock* [2005] has run a survey through 4.5 years (1996/04-2000/12) of solar wind data by ACE, IMP-8 and WIND and selected all time periods with existing upstream solar wind data where a single IMF B_y sign change takes place during constantly northward IMF at least 2 h before and 3 h after the B_y sign reversal. The possible occurrence of a TPA during such solar wind conditions is examined with the help of auroral images from Polar UVI. Because of the spacecraft orbit, a global view on the auroral zone during a significant fraction of time exists only for the northern hemisphere. We therefore concentrate on TPAs appearing in this hemisphere.

2.1. Polar UV Images

[17] The UV camera on Polar images the aurora every 37 s in the ultraviolet region of the spectrum using four narrow band filters with integration times of 18 and 36 s, respectively [*Torr et al.*, 1995]. In this study we use the LBH short (149–160 nm) and the LBH long (160–180 nm) filters with an integration time of 36 s. In the LBH long mode emissions are not significantly absorbed in the atmosphere, thus the emission intensity is approximately proportional to the electron energy flux into the ionosphere [*Germany et al.*, 1998]. However, this filter is less sensitive than the LBH short filter and does not resolve faint structures just above the instrument threshold very well. Although LBH short wavelengths generally suffer from absorption in the atmosphere, the resulting error becomes negligible for weak aurorae that are caused by low energy electrons [*Germany et al.*, 1998]. As predicted theoretically by *Germany et al.* [1990], the emissions of low energy electrons peak at high altitudes where absorption becomes negligible due to a rapid decrease of absorption with height [*Germany et al.*, 2001]. TPAs have often very faint structures, with luminosities near Polar UVIs threshold [*Kullen et al.*, 2002] and are typically caused by particles with low energies [*Frank et al.*, 1986]. Thus absorption in the LBH short mode should be negligible. We therefore measure the TPA luminosity in both wavelength ranges, and compare their results.

[18] The resolution of the UV imager on the Polar spacecraft is about 0.5° s in latitude at apogee: thus a single pixel projected to 100 km altitude from apogee is approximately 50×50 km. Away from apogee the imager can detect even smaller spatial scales. Because of a spacecraft wobble in one spacecraft direction, the effective pixel size

sometimes increase up to 50×250 km. This is of no consequence for our purpose.

[19] Dayglow is removed from sunlit images. For those events where a transparent MgF window was closed to protect the optics of the imager, the reduction of the image sensitivity is corrected. For more details see *Cumnock* [2005]. Only those cases (19 out of 55 time periods) were taken into account in their paper, where the entire evolution of a TPA can be followed on Polar UV images. In the present study, four additional events are included into the data set. These TPAs appear during the required solar wind conditions and form a true theta aurora, but are during part of their existence out of the view of the imager. As we are in this study not interested in the entire evolution of TPAs, these cases are taken into account as well. Those TPAs where both the transparent image window was closed and dayglow was removed due to sunlit conditions, are ignored in the study. The multiplication of both correction factors results in too large error bars. For this reason, one of the events presented by *Cumnock* [2005] has been excluded from the data set. Another event from the *Cumnock* [2005] list is removed, as it does not contain images in the LBH long mode. For all other TPAs, images in the LBH long wavelength range exist. The coverage in the LBH short mode is not as good. They are taken into account as far as they exist (15 cases). The study contains now altogether 21 events. Note, that the data set includes even two cases where an IMF B_y sign change takes place, but no TPA could be identified on Polar UVI or with DMSP particle data.

[20] The number of events seems small compared to the examined time period of 4.5 years. One reason is the need for global Polar UV images from the northern ionosphere during the time period of interest. The IMF selection criterion of a single IMF B_y sign reversal occurring during at least 5 h of steady northward IMF diminishes the number of possible events additionally. Solar wind conditions with extended intervals of northward IMF are rather rare and occur mainly in connection with magnetic clouds and their sheath fields. The sheath field consists of high magnetic fields, the ejecta itself is characterized by slowly varying magnetic fields, which often have a north-to-south (or vice versa) rotation to it [*Tsurutani and Gonzalez*, 1997]. Comparing our TPA list with the automatically generated list of CMEs and CME-like structures by *Lepping et al.* [1990] shows that 15 out of 21 TPAs occur within 16 h of the force-free part of the CME main ejecta. This means, the large majority of our IMF B_y sign reversal periods are part of a CME induced magnetic structure of the IMF.

[21] The intensity of the UV emissions is measured at the point in time when the TPA has reached the noon-midnight meridian, forming a true theta aurora. The maximum and minimum UV emissions along the arc (excluding the oval connection points) are determined by visual inspection of the UV images. Despite the use of a dayglow removal routine, for most summer TPAs the part of the oval near noon is not visible due to too much dayglow in that area. Thus luminosity measurements are taken at the visible part of the TPA only. Some TPAs have an extremely weak luminosity which makes it difficult to identify the arc at each point of time. In these cases, particle data from one of the dawn-dusk orbiting DMSP (Defense Meteorological

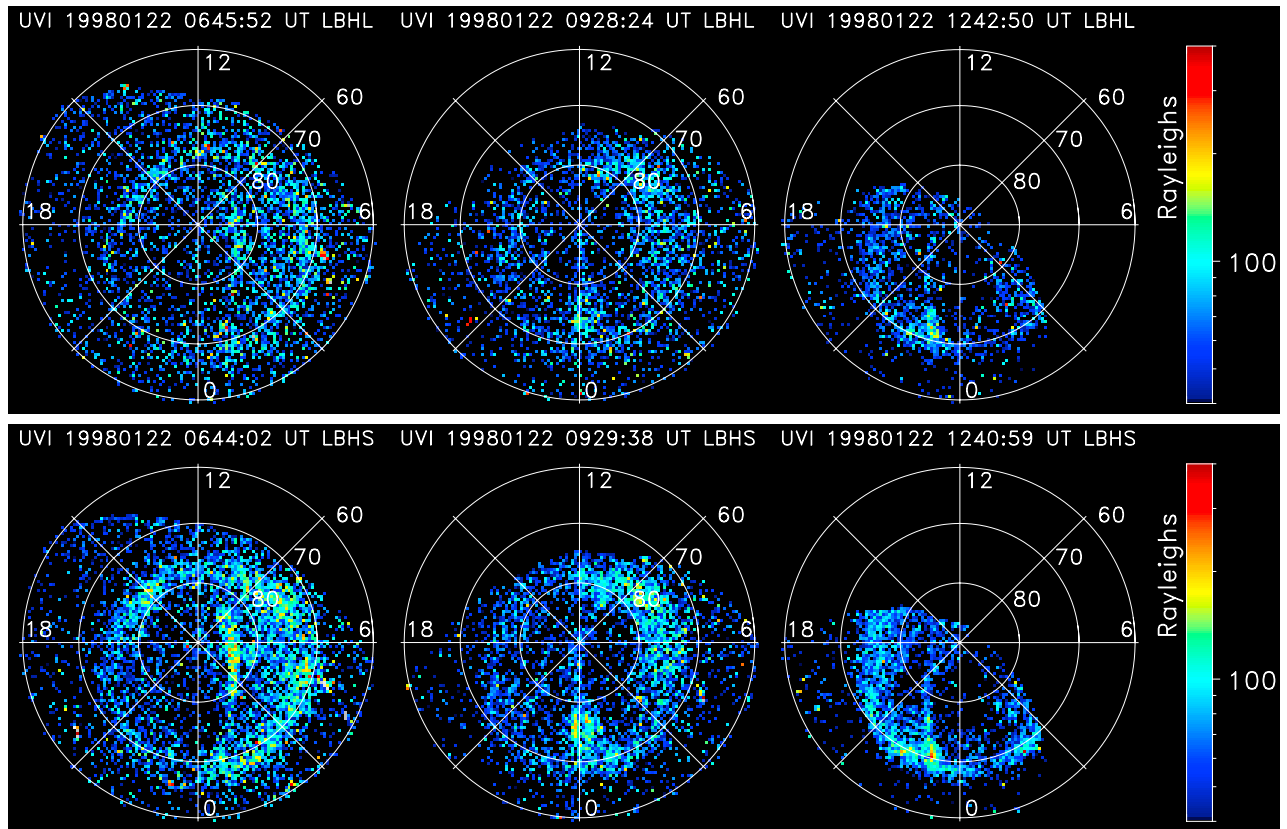


Figure 1. Example of a dawn-to-dusk moving transpolar arc, seen on Polar UVI in the LBH long mode (top row) and in the LBH short mode (bottom row).

Satellite Program) spacecrafts at 1000 km height are used to verify the exact position of the arc.

[22] As we are interested in the effect of solar illumination on the TPA luminosity, we sort the events into sunlit (positive Earth dipole tilt) and dark hemisphere cases (negative Earth dipole tilt). The terminator (at 100 km) separating the sunlit from the dark side of the ionosphere has been determined for each event. In the majority of cases, the entire arc lies completely in darkness or sunlight when the Earth dipole tilt is negative or positive, respectively. However, for four negative and two positive tilt events, the terminator divides the TPA into a small sunlight and a large dark part. This does not cause any problem in the negative tilt cases. The luminosity has been determined for the dark side only. In the positive dipole tilt cases the terminator is too close to the region that appears on the UV imager as completely covered by dayglow, such that a determination of the TPA luminosity in the sunlight region is not possible. Thus for these two cases, the luminosity values are taken on the dark side as well.

[23] An example of a TPA is shown in Figure 1 in the LBH long mode (top row) and in the LBH short mode (bottom row) of Polar UVI. It appears in the northern hemisphere on 22 January 1998. The Figure shows clearly the higher sensitivity of the LBH short filter. In that filter, the TPA is much easier discernable from the background noise than in the LBH long filter. The minimum and maximum auroral luminosity values are measured in both modes along the arc at 9:28 UT and 9:29 UT, respectively.

Around that time, the TPA has reached the noon-midnight meridian. During the event, the IMF is dominated by its B_z component. IMF B_z has high values above 10 nT and stays northward for over 30 h, while the IMF B_y changes three times its sign, each time triggering a TPA to move into the polar cap. The TPA shown in Figure 1 appears in connection with a last sign change from -5 to $+5$ nT, that leads to the separation of the TPA from the dawnside oval and its motion over the entire polar cap within 8.3 h.

2.2. Solar Wind Data

[24] For an examination of the solar wind conditions during the TPA events 1-min averaged OMNI data are used. It is provided on the OMNIWeb (<http://omniweb.gsfc.nasa.gov>). The data set consists of solar wind measurements from the solar wind monitor which is closest to the Earth bow shock. Hence near continuous measurements are provided. The data are propagated in time to correspond the solar wind conditions at the Earth bow shock. A detailed documentation is given by *King and Papitashvili [2005]*. The OMNI data used in our study consists of measurements from the satellites WIND, IMP-8, Geotail and ACE.

3. Results

3.1. TPA Luminosity

[25] The seasonal dependence of the TPA luminosity, reported already by *Cumcock [2005]*, is shown in Figure 2 for our extended TPA list. For each event, LBH short (left

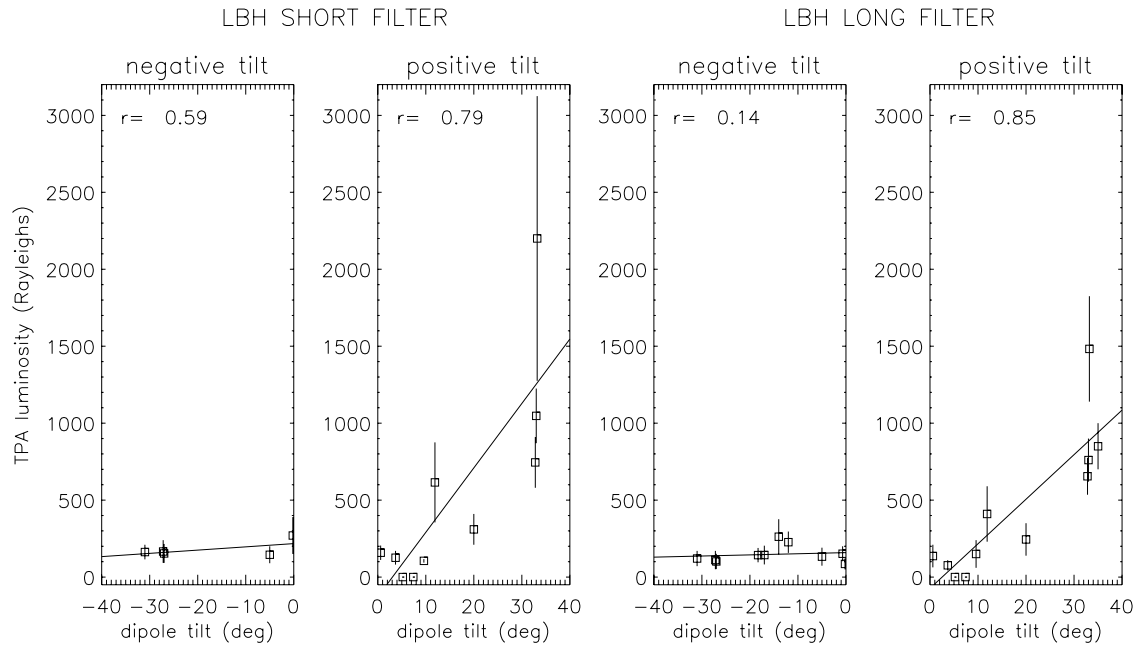


Figure 2. TPA luminosity measured with the LBH short filter (left two plots) and the LBH long filter (right two plots) versus Earth dipole tilt. The TPAs are sorted after negative and positive dipole tilts. The luminosity is measured when the arc has reached the noon-midnight meridian. The ends of each vertical line correspond to the minimum and maximum luminosity values. Linear regression lines and correlation coefficients are calculated for the average TPA luminosities, marked as squares at each vertical line.

side) and LBH long (right side) UV emissions (measured when the arc has reached the noon-midnight meridian) versus Earth dipole tilt are plotted. The cases with a negative (dark hemisphere) and a positive Earth dipole tilt (sunlit hemisphere) are shown in separate plots. Each vertical line corresponds to the luminosity range of one TPA. The upper and lower ends of the vertical lines correspond to the measured maximum and minimum values, respectively. The squares in the middle of each vertical line mark the average between these two values. They represent a quite good estimate of the real averaged TPA luminosity, as in most cases the minimum and maximum values do not deviate much from each other. For each plot the correlation coefficients and regression lines are calculated for the luminosity averages (marked as squares).

[26] Comparing the measurements taken with the LBH short filter with those from the LBH long filter, the results look quite similar. Disregarding the brightest TPA, the UV emissions are only slightly higher in the LBH short mode than for the LBH long mode. Most of the 21 TPAs have rather low luminosity values below 300 Rayleigh. With increasing luminosity, the difference between minimum and maximum values grows slightly. Only for the brightest TPA this difference becomes large. That event appears in connection with a magnetic storm recovery, resulting in a wide and bright oval.

[27] The global Polar UV images show that in most cases, not only the TPA but also the entire auroral oval is very faint (see example in Figure 1). The low luminosity values indicate a quiet state of the magnetosphere. A look at the AE index quicklook plots on the Kyoto WDC-WEB (<http://swdewww.kugi.kyoto-u.ac.jp/aedir/index.html>) confirms

this: Except for the storm recovery event all TPAs appear during time periods of absolute quietness or with only minor AE disturbances. As can be expected for such AE conditions, the TPA brightness does not vary much. A slightly enhanced nightside oval connection point is observed for three TPAs, brightenings along the arc are seen in six cases. However, when the TPA has reached the noon-midnight line (the time point of our UV emission measurements), all auroral intensifications have disappeared. Except for three cases where an auroral breakup occurs while the TPA starts to form, no substorm activity is observed. The nearly complete absence of substorm breakups in our data set has to do with the well-known decrease of substorm activity during extended periods of northward IMF [Kullen and Karlsson, 2004].

[28] Comparing the negative with the positive Earth dipole tilt cases of Figure 2, the dependence of the TPA luminosity on sunlight can be clearly seen: For negative dipole tilts the TPA luminosity is generally very low, and the auroral brightness does not depend on the dipole tilt. For positive dipole tilt angles the UV emissions are in average much higher. The good correlation with the dipole tilt angle shows that in the sunlit hemisphere the TPA brightness strongly depends on the Earth dipole tilt.

3.2. Correlation Between TPA Luminosity and Solar Wind Parameters

[29] To find out about a possible dependence of the TPA luminosity on solar wind conditions, we calculate correlation coefficients between the average TPA luminosity and different solar wind parameters. The average TPA luminosity is approximated by the mean value between minimum

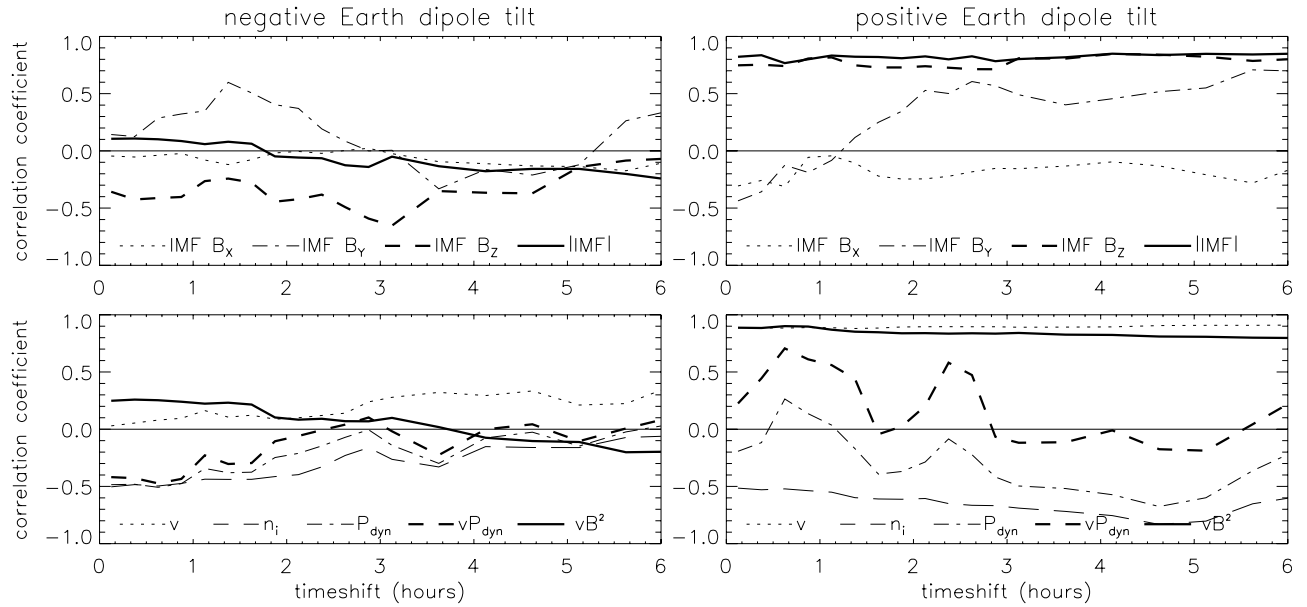


Figure 3. Correlation coefficients between TPA luminosity in the LBH long mode and solar wind parameters are shown for time shifts between luminosity measurements and solar wind values up to 6 h back in time. The correlation coefficients are calculated separately for events with negative (left plots) and positive dipole tilts (right plots). The top plots show the correlations with the IMF, the bottom plots give the dependence on solar wind speed, density, pressure, magnetic, and kinetic energy flux.

and maximum UV emissions at the time when the TPA has reached the noon-midnight meridian. The OMNI Web solar wind data are already shifted in time to correspond the solar wind conditions at the Earth's bow shock nose. We average the data over 15 min intervals because of the frequent occurrence of small data gaps, especially in the IMP-8 data. To get information about the time it takes until the solar wind influences the TPA brightness we calculate the correlation coefficients for solar wind values up to several hours before the TPA has reached the noon-midnight meridian. To take seasonal effects into account, we distinguish between TPAs that occur during sunlit and dark conditions.

[30] The solar wind correlation plots have been produced for both LBH long and LBH short values. As the LBH short filter is more sensitive, we expect to get more accurate luminosity values than with the LBH long filter (in 6 out of 15 cases where TPA images exist for both filters, the TPA is much better visible with the LBH short filter). However, in our study the results do not improve by using this filter. For negative Earth dipole tilt cases (containing very low UV emissions) no correlation with solar wind parameters is found, independent of which filter is used. For positive Earth dipole tilts (with slightly higher TPA luminosities), LBH short and LBH long correlation plots are nearly identical. This is the reason why the results are shown in Figures 3 and 4 only in LBH long.

[31] Figure 3 shows the correlation coefficients for the different solar wind parameters in the dark (left side) and the sunlit hemisphere (right side) for solar wind values 7.5 min up to 6 h before the TPA measurements were taken. The plots in the first row provide information about the IMF. The plots in the second row show the correlation coefficients for the solar wind bulk speed, the solar wind ion density, the dynamic pressure, and kinetic and magnetic energy fluxes.

[32] As mentioned above, a correlation between solar wind parameters and TPA is only found for the sunlit cases. The for all solar wind parameters very low correlation coefficient values for negative dipole tilts may indicate that the TPA luminosity is not influenced by solar wind or IMF. Alternatively, the weak UV emissions in the dark hemisphere may be too low to be correctly measured by the imager since their values are near the instrument threshold.

[33] In the sunlit hemisphere the TPA brightness is strongly influenced by several solar wind parameters: TPAs become brighter for increasing IMF magnitude, IMF B_z , and solar wind speed. For the solar wind density, a weak negative correlation with the TPA luminosity is observed. The solar wind pressure has no influence on the TPA luminosity. Previous studies indicate an anticorrelation with IMF B_x . This result is not confirmed in our data set. The correlation coefficient is constantly negative, but much too low to confirm a connection between TPA luminosity and negative IMF B_x .

[34] The results for IMF B_y have to be interpreted with care as the events have been selected to contain all a single B_y sign change. The correlation between TPA luminosity and IMF B_y is negative during the theta formation. For time shifts greater than 75 min, the correlation shows positive values. This is connected to the IMF B_y sign change that has taken place in average about 90 min before the theta formation is reached. The curve tells us that TPAs following a sign change from positive to negative are usually brighter than TPAs occurring after a B_y sign reversal from negative to positive.

[35] The magnetic energy flux of the solar wind has a much stronger influence on the TPA brightness than the kinetic energy flux. It has a maximal correlation coefficient of 0.9. The correlation coefficients for other known solar wind coupling functions such as $vB_z, v\sqrt{(B_y^2 + B_z^2)}$, or the transverse

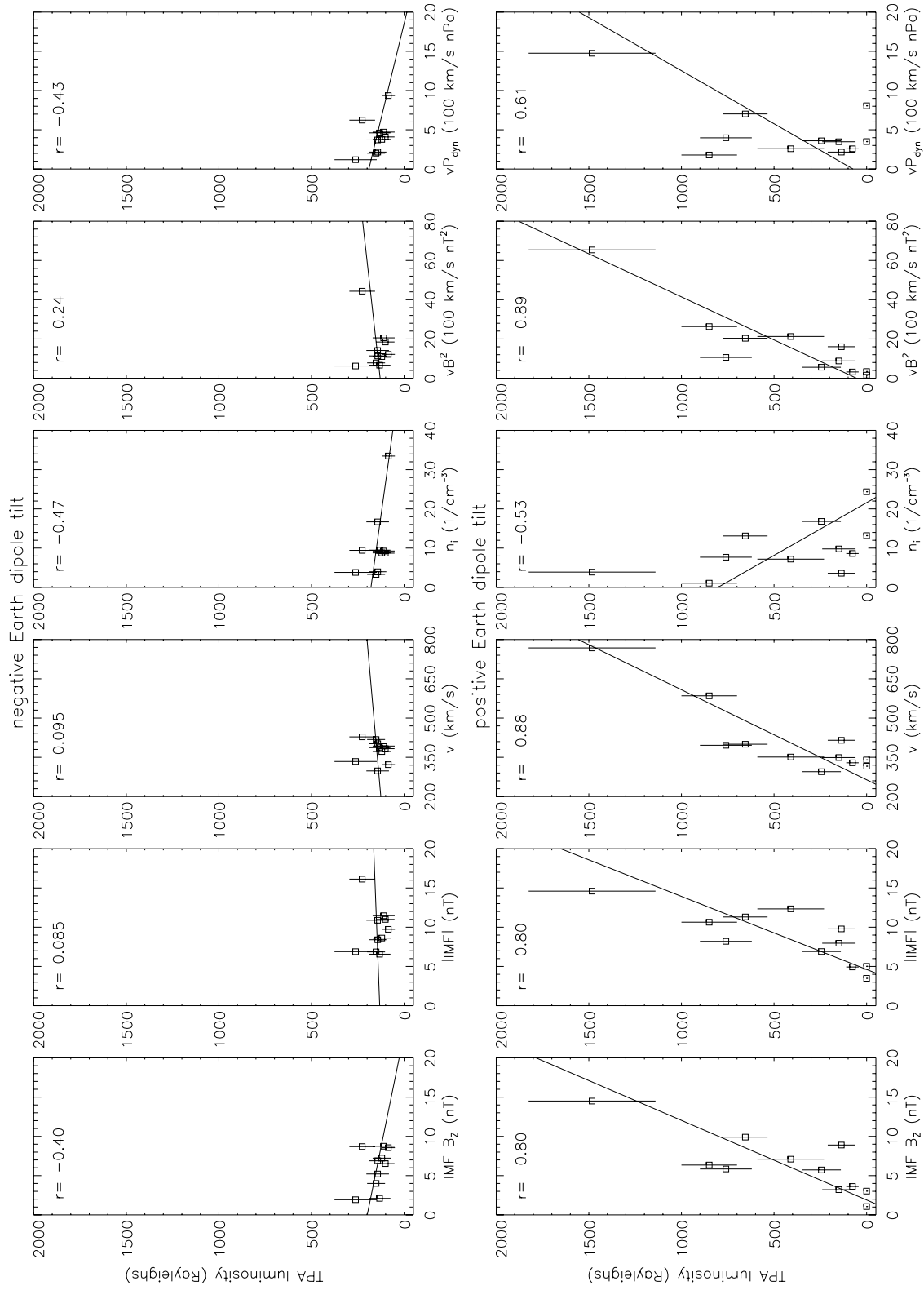


Figure 4. TPA luminosity (measured in the LBH long wavelength range) versus different solar wind parameters. The IMF and solar wind values are averaged over a 15 min time interval, between 60 and 45 min before the TPA has reached the noon-midnight line. The plots are produced in the same way as Figure 2.

component of the solar wind electric field ($v \times B$) give equally good results as the magnetic energy flux. They are not shown here as the only small deviations between these makes a detailed comparison meaningless for such a small data set.

[36] Looking at the shape of the curves for the sunlit hemisphere events, it is astonishing how little the correlation coefficients change in time for most parameters. Apparently, it is difficult to deduce an exact propagation time for the given TPA list. This has to do with the selection criteria of the events: The CME or CME-like structures during which the majority of these TPAs occur are connected to extremely stable solar wind conditions that change slowly within hours. Disregarding the IMF B_y correlation curve (result biased by the selection criterion), only the correlation with solar wind pressure and (connected) kinetic energy flux vary clearly for different time lags. For the kinetic energy flux, a maximal correlation of 0.7 is reached for a time lag of about 40 min.

3.3. Strength of Solar Wind Influence on TPA Luminosity

[37] While Figure 3 provides information about how well the TPA brightness correlates with different solar wind parameters, it does not tell us about how strong the different parameters influence the TPA luminosity. This is shown in Figure 4 for those parameters where a clear correlation with the TPA brightness was found. The TPA luminosity is plotted versus IMF B_z , IMF magnitude, solar wind velocity, ion density, magnetic and kinetic solar wind energy flux. The plots are done in the same way as Figure 2. The TPAs are sorted into cases with a negative Earth dipole tilt (upper row) and cases with a positive dipole tilt (lower row). For each plot, correlation coefficients and linear regression lines are calculated for the average TPA luminosity values (marked as squares). The solar wind data are averaged over a 15 min time interval between 45 and 60 min before the TPA reaches the noon-midnight meridian. As discussed above, the exact time shift does not matter. Except for the kinetic energy flux (which has nearly maximal correlation values for the plotted time shift) the results do not change considerably within some tens of minutes for the shown parameters.

[38] As already seen in Figure 3, a clear dependence of the TPA luminosity on solar wind and IMF is found only for the sunlit cases. Figure 4 shows that not only is the correlation very high, but also the regression line is quite steep during sunlit conditions. The best correlations are found for the solar wind speed and the magnetic energy flux. From Figure 4 we can see that this correlation holds even for the most extreme cases. For the two cases with the lowest solar wind energy flux values, no TPA could be identified on Polar UV and DMSP data. The TPA which occurs during a magnetic storm with extremely high solar wind energy flux values is also the brightest one.

3.4. Intercorrelations of Solar Wind Parameters

[39] As all events appear during similar solar wind conditions (most of them in connection with CMEs or CME-like structures), the different solar wind parameters may be correlated with each other. To analyze this, Figure 5 shows the relation between IMF magnitude and each IMF component, solar wind speed, density and pressure. The plots are done in the same way and for the same time interval as Figure 4.

[40] Figure 5 reveals that the IMF has unusually high values, and is dominated by its north-south component, a typical characteristics of CMEs. Consequently, a very high correlation between IMF B_z and IMF magnitude is found. As could be expected, no correlation is found between IMF magnitude and the B_y component (due to the event selection criterion). For all other parameters, the correlations for the sunlit and dark hemisphere deviate from each other. For the dark hemisphere, the IMF magnitude depends only on IMF B_x and B_z . In the summer hemisphere, there is a clear, positive correlation between IMF magnitude and solar wind speed and a negative correlation with the solar wind density.

[41] For the sunlit hemisphere events, the correlations between IMF magnitude and solar wind parameters (Figure 5) are very similar to the correlations found between UV emissions and solar wind parameters (Figure 4). The question arises, to what extent the correlations found between TPA luminosity and solar wind velocity or density are caused by solar wind intercorrelations (correlations between IMF magnitude and solar wind velocity or density) rather than expressing a general dependence of the auroral luminosity on these parameters.

4. Discussion

4.1. TPA Luminosity Measurements Using Different LBH Wavelength Ranges

[42] The comparison of TPA luminosity values measured in the LBH short and LBH long wavelength ranges shows that both filters give very similar results (Figure 2). Only for the brightest TPA, LBH long and short measurements deviate strongly. As it is generally observed that TPAs have low particle energies [e.g., *Frank et al.*, 1986], we assume that the low UV emissions of our faint TPAs are caused by low energetic electrons. Assuming this, our results confirm the theoretical predictions by *Germany et al.* [1990, 2001] that low energy electrons appear at such high altitudes, that LBH short absorption can be neglected.

4.2. Seasonal Dependence of TPA Luminosity

[43] As can be seen in Figure 2, TPAs are on average much brighter in the sunlit hemisphere than in the dark hemisphere. As the luminosity values for TPAs in the sunlit (dark) hemisphere have been determined along the sunlit (dark) side of the TPA only (except in two cases), Figure 2 shows directly the influence of solar illumination of the brightness of TPAs. A seasonal dependence of the TPA luminosity has already been reported by *Cumnock* [2005], but was not discussed there in further detail. We pick up at this point and try to give our understanding of the sunlight enhancement of the TPA luminosity:

[44] The suppression of aurora in sunlight, as observed by *Newell et al.* [1996], holds only for discrete arcs connected to high-energetic electron beams that appear mainly in the low-conductivity region of the premidnight oval. As reported by *Liou et al.* [2001] and *Shue et al.* [2001b] the remaining parts of the auroral oval show the opposite dependence on sunlight. *Shue et al.* [2001a] and *Ohtani et al.* [2005] explain the positive correlation between auroral luminosity and sunlight by a linear dependence of FACs on the ionospheric conductivity which implies a voltage generator in the source region [*Fujii and Iijima*, 1987]. An enhancement of the

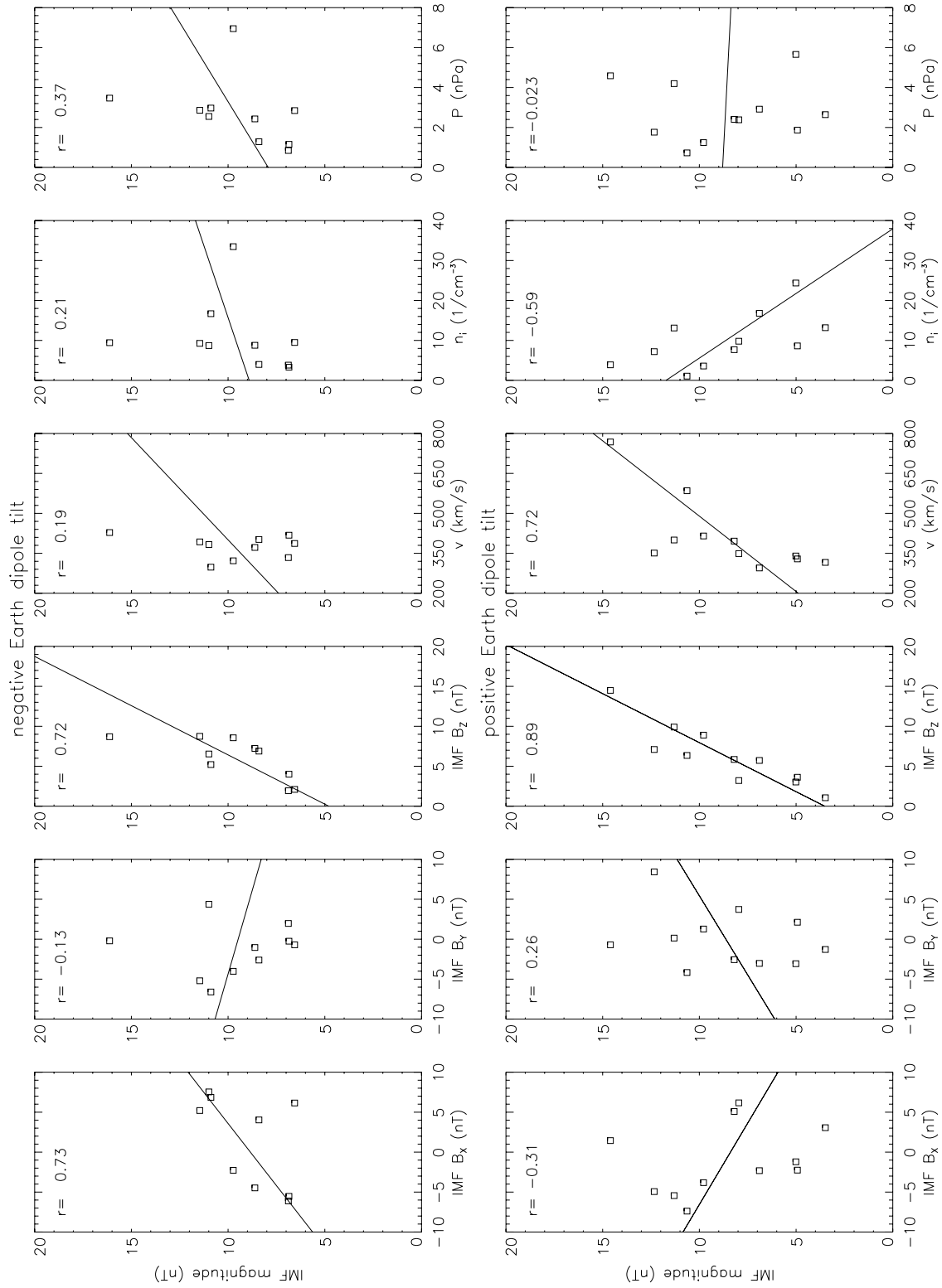


Figure 5. IMF magnitude versus different solar wind parameters for the same time interval as in Figure 4. The plots are produced in the same way as Figure 2.

ionospheric conductivity in sunlight leads thus to an enhancement of the aurora. The TPA luminosity shows the same seasonal dependence as the main auroral oval, away from the nightside sector. Thus it is probable that even TPAs are driven by a voltage generator.

[45] The explanation for the positive correlation between ionospheric conductivity and auroral brightness is based on the assumption that the aurora is diffuse. In that case the conductance is sufficient to satisfy the FAC requirement, resulting in weaker parallel E-fields and no discrete arcs. TPAs have been repeatedly observed to consist of discrete arcs [e.g., Frank *et al.*, 1986]. On the other hand, Hoffman *et al.* [1985] reported a TPA where no sign of electron acceleration occurred. Kullen *et al.* [2002] observed that TPA's can become extremely weak or even disappear during shorter time intervals on Polar UV images. Unfortunately, the pixel resolution of Polar UVI is not high enough to discern between discrete and diffuse aurora. However, these observations indicate that TPAs do not necessarily consist of discrete arcs during their entire existence. As our data set consists of TPAs appearing after hours of steady northward IMF with very low UV emissions in most cases, it is probable that diffuse aurora dominates in these cases, which would explain their similar dependence on season as the dayside oval. A detailed analysis of particle data from DMSP is planned to shed more light on this issue.

4.3. Comparison With Other Luminosity Studies

[46] Searching for a solar wind dependence of the TPA luminosity by looking at the entire TPA data set, does not give any clear results [Cumnock, 2005]. Only by separating TPAs appearing in the sunlit hemisphere from those of the dark hemisphere, clear dependencies on solar wind and IMF are found for the sunlit cases.

[47] Figures 3 and 4 show that the correlations between TPA luminosity and solar wind are much higher, and the dependence on the different parameters much stronger in the sunlit hemisphere than in the dark hemisphere. In fact, for negative dipole tilts, we did not find any clear connection between TPA luminosity and solar wind parameters. This is not confirmed by other studies. On the contrary, a similar dependence on solar wind parameters as for the sunlit cases is expected. Baker *et al.* [2003] observed for the northward IMF periods during one winter month similar solar wind dependencies for the polar cap and large parts of the main oval as our study for TPAs in the sunlit hemisphere. They show positive correlations with IMF B_z and solar wind speed, and negative correlations for IMF B_x and solar wind density. This may indicate that the sensitivity of the LBH long filter is not high enough to measure correctly the small differences in the UV emissions of the typically extremely faint winter TPAs of our study. Unfortunately, the number of dark hemisphere events taken with the more sensitive LBH short filter was too small to see any possible correlations. On the other hand, we have to consider that the luminosity study of Baker *et al.* [2003] was carried out for January 1997, a winter month with an extremely strong magnetic storm containing a long northward IMF phase with unusually bright and active aurora and many polar arcs during the northward storm phase. This would support the scenario that a strong solar wind influence on auroral lumi-

osity may be possible during the winter only above a certain level of solar wind energy input into the magnetosphere.

[48] For the sunlit hemisphere events, the correlations between TPA luminosity and different solar wind parameters, shown in Figures 3 and 4, resemble the correlations reported for the average auroral luminosity outside the nightside oval sector. This includes the very good correlations with northward IMF, the transverse component of the solar wind E-field, the magnetic solar wind energy flux, and a weak negative correlation with IMF B_x in the afternoon oval sector [Liou *et al.*, 1998], a negative correlation with IMF B_y [Shue *et al.*, 2001b] and positive correlation with solar wind velocity along the main oval [Shue *et al.*, 2002; Baker *et al.*, 2003]. Although not addressed by the authors, in the work of Shue *et al.* [2002] it can be seen that the connection between solar wind density and auroral luminosity in the polar cap is similar to our results for the TPA luminosity. During northward IMF a negative dependence on the density can be observed for the summer hemisphere.

[49] It is well-known that aurorae in the southern and northern hemisphere are influenced differently by IMF B_x . Not only the auroral luminosity [Liou *et al.*, 1998] also the occurrence frequency of polar arcs is correlated with IMF B_x . Small-scale [Valladares *et al.*, 1994], large-scale polar auroral arcs [Kullen *et al.*, 2002], and HiLDAs [Frey *et al.*, 2004] appear in the northern hemisphere most frequently during negative IMF B_x . In the southern hemisphere a correlation between NBZ current density and positive IMF B_x is found [Iijima *et al.*, 1984]. The asymmetric effect of IMF B_x on auroral luminosity, polar arc occurrence and FACs in the polar cap has been explained by most authors with more favorable conditions for high-latitude lobe reconnection due to highly antiparallel B-fields for negative (positive) IMF B_x in the southern (northern) hemisphere.

[50] A positive Earth dipole tilt has the same effect on the high-latitude reconnection topology in the northern hemisphere as negative B_x . For a sunward tilt of the north part of the Earth dipole axis, IMF and magnetospheric magnetic fields become more antiparallel in the northern hemisphere. Thus it could be expected, that the TPA luminosity depends as much on IMF B_x as on season. However, comparing Figures 2 and 3, we find that the influence of IMF B_x is negligible as compared to the effect of the Earth dipole tilt on TPA luminosity. A similar observation has been made by Crooker and Rich [1993] regarding the influence of IMF B_x and Earth dipole tilt on the average ionospheric convection pattern. They reported that the dipole tilt effect completely dominates over the B_x effect on the ionosphere. This is probably connected to the dipole tilt controlled UV illumination of the high-latitude ionosphere, and thus its influence on the ionospheric conductivity. The stronger dependence of the TPA brightness on the dipole tilt lets us suggest that sunlight has a much stronger influence on the TPA luminosity than a favorable reconnection topology.

[51] The independence of the TPA luminosity on the solar wind pressure (Figure 3) has been reported for other auroral regions as well. Neither for the afternoon oval [Liou *et al.*, 1998] nor for the polar cap aurora in the winter hemisphere [Baker *et al.*, 2003] a connection with the solar wind pressure has been found. Only Shue *et al.* [2002] find a weak, negative dependence of auroral luminosity in the

polar cap on pressure during the summer season. It is well-known that a sharp increase of the solar wind pressure causes within minutes a brightening of the noon aurora which spreads along the oval [Elphinstone *et al.*, 1991], and may even lead to an intensification of a TPA [Liou *et al.*, 2005]. The sudden compression of the magnetosphere by shock impact probably causes more particles to enter the loss cone although the exact mechanism is not known. Zhou and Tsurutani [1999] suggested that it is connected to wave-particle scattering, [Liou *et al.*, 2005] proposed a temporal widening of the loss cone due to a magnetic field line reconfiguration as a possible explanation for the auroral enhancement. Whatever the reason, apparently a rapid pressure jump may enhance the brightness of a TPA for a short time interval [Liou *et al.*, 2005] while a constantly high solar wind pressure level has no influence on the TPA luminosity or on the average auroral brightness along the oval. Thus the rate of increase or decrease, not the magnitude of the pressure is important for a change in the auroral luminosity.

4.4. Intercorrelations of Solar Wind Parameters

[52] From Figure 5 we know that in the sunlit hemisphere, the correlations between IMF magnitude and other solar wind parameters resemble the correlations between TPA luminosity and solar wind parameters. Because of this similarity, it cannot be ruled out that the positive (negative) correlation between TPA luminosity and solar wind speed (density) may be a secondary dependency arising from the internal solar wind correlations and that neither the solar wind speed nor its density have a direct influence on the strength of the UV emissions. It could also be that the TPA brightness is mainly controlled by the solar wind speed. Both parameters, IMF magnitude and solar wind velocity show very high correlations with the UV emissions of TPAs.

[53] On the other hand, the similarity between our results and the dependencies found for the auroral luminosity in major parts of the main oval [Liou *et al.*, 1998; Shue *et al.*, 2002; Baker *et al.*, 2003] indicates that the solar wind and IMF dependence of the TPA luminosity may be valid more general. Note, that both Liou *et al.* [1998] and Baker *et al.* [2003] tested possible solar wind intercorrelations in their data sets and found no correlations that would explain the enhancement of the auroral luminosity during northward IMF for high solar wind velocity or low solar wind density. Thus their results are not biased by the solar wind distribution during the covered time period.

4.5. Dipole Tilt Influence on Conjugate Transpolar Arcs

[54] MHD simulations [e.g., Slinker *et al.*, 2001; Kullen and Janhunen, 2004] and observations [Obara *et al.*, 1988; Craven *et al.*, 1991] clearly show that TPAs triggered by an IMF B_y reversal occur simultaneously on both hemispheres, but with opposite dawn-dusk motion. From Cumnock [2005] and this study we know that the TPA luminosity strongly depends on the Earth dipole tilt. This would mean that for large Earth dipole tilts, the TPA in the sunlit hemisphere would be much brighter than the arc appearing in the opposite hemisphere.

[55] Observations about this subject are rather confusing so far. Our study shows that the dipole tilt angle has an influence on the TPA luminosity while the IMF B_x compo-

nent has no influence. In opposite to what could be expected from our results, Ostgaard *et al.* [2003] observed a TPA occurring after an IMF B_y sign change in the southern hemisphere, while no (at least not very clear) TPA was visible in the northern hemisphere. During that event, both, IMF B_x and Earth dipole tilt were positive. As pointed out by Ostgaard *et al.* [2003], apparently the IMF B_x effect dominated over the Earth dipole tilt in that case. The clearly visible TPA appeared in the dark hemisphere, not in the sunlit hemisphere. Further investigations would be necessary to find out which parameter plays the dominant role and whether there are other mechanisms to suppress TPAs in one of the hemispheres.

4.6. Propagation Time Between Solar Wind and TPAs

[56] As seen in Figure 3 for the sunlit cases, the correlation coefficients change very little with time for those solar wind parameters that show a strong correlation with the TPA luminosity. Thus an optimal time shift between solar wind and TPA luminosity cannot be determined from these parameters. As mentioned above, this is connected to the only small variations of these parameters during a CME event. Disregarding the curve for IMF B_y (its shape is connected to the B_y sign change selection criterion) only the correlations with the pressure and the kinetic energy flux vary for different time shifts. While the correlation coefficient values for the pressure are very low for all time shifts, a dependence on the kinetic energy flux is found for time shifts between 30 and 60 min. The time shift for which the highest correlation with the kinetic energy flux occurs (about 40 min) should correspond to the time needed for changed kinetic energy flux values to affect the TPA luminosity.

[57] A propagation time of 40 min is in the same order of magnitude as the by Liou *et al.* [2005] observed time delays between 10 and 65 min until a sudden solar wind pressure jump cause a brightening along a TPA. In their example, an auroral intensification starts nearly instantly after a sharp solar wind pressure increase at the dayside oval and spreads then along the oval to the nightside before the TPA brightens as well. The reason for such a long time delay is the far tail origin of the TPA. The similar particle characteristics of main oval and TPA indicates that both lie on closed field lines [e.g., Frank *et al.*, 1986]. The main difference is the much further poleward location of the TPA which means a much further tailward origin. As shown by Kullen and Janhunen [2004] a TPA maps to the most tailward part of the closed field line region that has become extremely expanded in tailward direction after the IMF B_y sign change. The source region of the main auroral oval lies Earthward of it, which explains why the main oval brightens before the TPA does [Liou *et al.*, 2005]. Assuming an average solar wind speed of 400 km/s, a time delay of 40 min would mean that the closed field line region extends $150 R_e$ downtail during the evolution of a TPA.

4.7. Connection Between TPA Luminosity and TPA Occurrence Frequency

[58] The solar wind conditions during which bright TPAs appear in the sunlit hemisphere, are similar to the conditions for which a high occurrence frequency of TPAs is expected. Makita and Meng [1989], as well as Kullen *et al.* [2002] observed that TPAs (denoted as moving arcs in the work of

Kullen et al. [2002]) appear most commonly for large IMF magnitudes and high solar wind speed. Furthermore, *Kullen et al.* [2002] found a strong positive correlation with northward IMF and a negative correlation with IMF B_x . No dependence on the solar wind pressure, and in opposite to our study, no dependence on the solar wind density is seen. Note that *Kullen et al.* [2002] checked the internal solar wind relations during the studied period of three winter months, and found no correlation between IMF magnitude and solar wind velocity or density, i.e., the observed solar wind dependencies are not biased.

[59] The occurrence frequency of large-scale polar arcs was shown by *Kullen et al.* [2002] to correlate best with a function, called anti-epsilon $\sim \nu B^2 \cos^4(\frac{\theta}{2})$. The clock angle θ is defined as the angle between the projection of the IMF vector on the yz -plane and the positive z axis ranging from 0° for pure northward to 180° for pure southward IMF. This means basically, polar arcs appear most commonly for a high solar wind energy flux during northward IMF conditions. A similar function, $\epsilon^* = B_y^2 + B_z^{2(0.5)} \cos(\frac{\theta}{2})$

was inferred by *Iijima et al.* [1984] as it correlates well with the current density of the dayside NBZ currents in the polar cap. Unfortunately, it is not possible to study the influence of these solar wind coupling functions on the TPA luminosity as the role of the IMF clock angle cannot be examined here. Because of the selection criterion of a single IMF B_y sign change during northward IMF, the IMF clock angle values are nearly identical for all events. However, we know that the magnetic energy flux strongly influences TPA occurrence frequency [*Kullen et al.*, 2002]. Probably, the low occurrence rate of TPAs for low values of the solar wind magnetic energy flux is connected to the extremely low TPA luminosity during such solar wind conditions. The best example for this assumption is the observation that of all 21 B_y sign change cases studied here, TPAs were absent in only those two cases where the solar wind energy flux had lowest values.

[60] *Kullen* [2000] suggested that the spatial evolution of TPAs can be sufficiently explained by the large-scale topological changes in the magnetotail caused by an IMF B_y sign change during northward IMF. This semianalytical model was later on confirmed by several MHD simulations [*Slinker et al.*, 2001; *Kullen and Janhunen*, 2004; *Naehr and Toffoletto*, 2004]. *Kullen and Janhunen* [2004] showed in detail that such solar wind conditions lead to a rotation of a twisted magnetotail that starts at the flanks of the near-Earth region and propagates then inward and downtail such that during an intermediate state, near-Earth and far tail are oppositely twisted. The region of closed field lines becomes strongly deformed and tailwardly stretched during this transformation period. Mapping from the tail plasma sheet to the Earth results into a bifurcation of the closed field line region in both hemispheres. The most tailward part of the closed field line region maps to a ‘finger’ moving from one oval side to the other, but in opposite direction for northern and southern hemisphere. Assuming TPAs lie on closed field lines [*Frank et al.*, 1986] the ionospheric end of the bifurcated closed field line strip corresponds to the location of the TPA.

[61] While the expected motion of the bifurcated closed field line strip over the entire polar cap occurs in the

simulations, the MHD models are not good enough to recreate fine-scale FAC structures in the polar cap. In the study by *Kullen and Janhunen* [2004], no FACs occur poleward of the main oval, in the work of *Naehr and Toffoletto* [2004], FACs occur during a few minutes, but do not coincide with the bifurcated closed field line strip. Hence strength and origin of FACs causing the TPA, cannot be analyzed with MHD simulations and no conclusions can be drawn regarding the brightness of TPAs.

[62] The results of this study help to close this gap: The similar dependence of TPA frequency and luminosity on solar wind conditions combined with the above described MHD results, lets us conclude that the magnetic topology necessary for the development of TPAs always occurs after an IMF B_y reversal during northward IMF. However, during solar wind conditions with an extremely low magnetic energy flux, the aurora is not bright enough to be detected on global auroral imagers, alternatively the FAC connected to the bifurcated closed field line region are too weak to produce aurora.

[63] It should be pointed out that most TPAs do not occur during as ideal conditions as the ones selected for this study: Auroral breakups, caused by internal magnetospheric instabilities such as substorm onsets (often in connection with IMF southturns), or pressure pulse related auroral brightenings influence the brightness of TPAs as well. The latter mechanisms cause much stronger, and more varying auroral light than continuously strong, northward IMF and a high solar wind speed.

5. Summary and Conclusions

[64] A unique set of TPAs, all occurring after an IMF B_y sign reversal during constantly northward IMF is examined with respect to a possible connection between auroral brightness and solar wind conditions.

[65] As reported by *Cumnock et al.* [1997] and more clearly shown by *Cumnock* [2005] such solar wind conditions trigger the separation of a large-scale auroral arc from one side of the oval which moves then across the polar cap. When having reached the noon-midnight meridian, it has transformed into a true theta aurora, spanning from the nightside oval until its dayside part. The brightness of the TPA is measured at this stage of its development.

[66] Due to the requirement of at least 5 h constantly northward IMF around the IMF B_y sign change, auroral breakups are nearly entirely suppressed, and the TPA brightness varies hardly along the arc. Note, that this is not very common: polar arcs often show strong luminosity variations, and auroral intensifications that appear frequently at the oval connection point often spread along the arc [*Kullen et al.*, 2002]. Thus the selected TPAs represent a unique data set: the solar wind influence on the TPA luminosity can be studied without dilution of substorms or other auroral intensifications that typically appear during southward or near zero IMF B_z conditions [*Kullen and Karlsson*, 2004].

[67] The influence of season and solar wind conditions on the average auroral luminosity of the main oval have been studied extensively in previous studies. With the present work, we are able to add information about the luminosity of auroral arcs inside the polar cap:

[68] The brightness of TPAs occurring after an IMF B_y sign change during constantly northward IMF shows the same dependence on season as the dawn-, dusk-, and dayside part of the main oval: Sorting the TPA events after the sign of the Earth dipole tilt, shows that TPAs are in average much brighter in the sunlit hemisphere than in the dark hemisphere [see also *Cumnock, 2005*]. TPAs that appear in the sunlit hemisphere are influenced by IMF and solar wind in a similar way as the aurora in the main oval, away from the nightside sector: high solar wind speed, strongly northward IMF, high IMF magnitude, and low solar wind density increase the TPA brightness considerably. IMF B_x , solar wind pressure, and the kinetic energy flux seem to have an only marginal influence. The TPA brightness is mainly determined by the magnetic energy flux of the solar wind. The reason why no correlation with solar wind parameters is found for the negative dipole tilt cases is probably connected to the very low TPA luminosity in the dark hemisphere. The weak UV emissions cannot be resolved very well, as they are close to the instrument threshold of the Polar UV imager.

[69] These results combined with observations that an IMF B_y sign reversal during northward IMF is connected to the occurrence of a TPA [*Cumnock, 2005*], that the probability to observe a TPA is high when the magnetic energy flux is large [*Kullen et al., 2002*], and MHD simulations results showing that the spatial evolution of an IMF B_y change triggered TPA is enforced by large-scale topological changes in the magnetotail [*Kullen and Janhunen, 2004*], leads us to suggest the following scenario: An IMF B_y change during northward IMF always causes a magnetospheric topology that makes the occurrence and motion of a TPA possible, but a certain amount of energy input into the magnetospheric system is necessary for the aurora to be visible on global auroral imagers, alternatively, for aurora to occur at all. Because of the dependence of the ionospheric conductivity on solar illumination, the TPA luminosity is also strongly influenced by the angle of the Earth dipole tilt.

[70] **Acknowledgments.** The authors thank George Parks and the Polar UVI team for providing UV images, as well as the ACE, IMP-8, and Wind instrument teams for providing magnetometer and plasma data through the GSFC/SPDF OMNIWeb interface at <http://omniweb.gsfc.nasa.gov>. Work at the University of Texas at Dallas was supported by NSF grant ATM0536868.

[71] Wolfgang Baumjohann thanks Lie Zhu and another reviewer for their assistance in evaluating this paper.

References

- Akasofu, S.-I. (1980), The solar wind-magnetosphere energy coupling and magnetospheric disturbances, *Planet. Space Sci.*, **28**, 495.
- Atkinson, G. (1970), Results of the interaction of a dynamic magnetosphere with the ionosphere, *J. Geophys. Res.*, **75**, 4746.
- Baker, J. B., A. J. Ridley, V. O. Papitashvili, and C. R. Clauer (2003), The dependence of winter aurora on interplanetary parameters, *J. Geophys. Res.*, **108**(A4), 8009, doi:10.1029/2002JA009352.
- Chang, S.-W., et al. (1998), A comparison of a model for the theta aurora with observations from Polar, Wind and SuperDARN, *J. Geophys. Res.*, **103**, 17,367.
- Craven, J. D., J. S. Murphree, L. A. Frank, and L. L. Cogger (1991), Simultaneous optical observations of transpolar arcs in the two polar caps, *Geophys. Res. Lett.*, **18**, 2297.
- Crooker, N. U., and F. J. Rich (1993), Lobe cell convection as a summer phenomenon, *J. Geophys. Res.*, **98**, 13,403.
- Cumnock, J. A. (2005), High-latitude aurora during steady northward interplanetary magnetic field and changing IMF B_y , *J. Geophys. Res.*, **110**, A02304, doi:10.1029/2004JA010867.
- Cumnock, J. A., J. R. Sharber, M. R. Hairston, R. A. Heelis, and J. D. Craven (1997), Evolution of the global auroral pattern during positive IMF B_z and varying IMF B_y conditions, *J. Geophys. Res.*, **102**, 17,489.
- Cumnock, J. A., J. R. Sharber, R. A. Heelis, L. G. Blomberg, G. A. Germany, J. F. Spann, and W. R. Coley (2002), Interplanetary magnetic field control of the theta aurora development, *J. Geophys. Res.*, **107**(A7), 1108, doi:10.1029/2001JA009126.
- Dungey, J. W. (1961), Interplanetary magnetic field and the auroral zones, *Phys. Rev. Lett.*, **6**, 47.
- Elphinstone, R. D., J. S. Murphree, L. L. Cogger, D. Hearn, M. G. Henderson, and R. Lundin (1991), Observations of changes to the auroral distribution prior to substorm onset, in *Magnetospheric Substorms*, *Geophys. Monogr. Ser.*, vol. 64, edited by J. Kan et al., 257 pp., AGU, Washington, D. C.
- Frank, L. A., et al. (1986), The theta aurora, *J. Geophys. Res.*, **91**, 3177.
- Frey, H. U., N. Ostgaard, T. J. Immel, H. Korth, and S. B. Mende (2004), Seasonal dependence of localized, high-latitude dayside aurora (HiLDA), *J. Geophys. Res.*, **109**, A04303, doi:10.1029/2003JA010293.
- Fujii, R., and T. Iijima (1987), Control of the ionospheric conductivities on large-scale Birkeland current intensities under geomagnetic quiet conditions, *J. Geophys. Res.*, **92**, 4505.
- Germany, G. A., M. R. Torr, P. G. Richards, and D. G. Torr (1990), The dependence of modeled OI 1356 and N2 Lyman Birge Hopfield auroral emissions on the neutral atmosphere, *J. Geophys. Res.*, **95**, 7725.
- Germany, G. A., J. F. Spann, G. K. Parks, M. J. Brittnacher, R. Elsen, L. Chen, D. Lummerzheim, and M. H. Rees (1998), Auroral observations from the POLAR Ultraviolet Imager (UVI), in *Geospace Mass and Energy Flow: Results from the International Solar-Terrestrial Physics Program*, *Geophys. Monogr. Ser.*, vol. 104, edited by J. L. Horwitz, D. L. Gallagher, and W. K. Peterson, p. 149, AGU, Washington, D. C.
- Germany, G. A., D. Lummerzheim, and P. G. Richards (2001), Impact of model differences on quantitative analysis of FUV auroral emissions: Total ionization cross section, *J. Geophys. Res.*, **106**, 12,837.
- Gussenhoven, M. S. (1988), Low-altitude convection, precipitation, and current patterns in the baseline magnetosphere, *Rev. Geophys. Space Phys.*, **26**, 792.
- Hoffman, R. A., R. A. Heelis, and J. S. Prasad (1985), A sun-aligned arc observed by DMSP and AE-C, *J. Geophys. Res.*, **90**, 9697.
- Iijima, T., T. A. Potemra, L. J. Zanetti, and P. F. Bythrow (1984), Large-scale Birkeland currents in the dayside polar region during strongly northward IMF: A new Birkeland current system, *J. Geophys. Res.*, **89**, 7441.
- Kessel, R. L., S.-H. Chen, J. L. Green, S. F. Fung, S. A. Boardsen, L. C. Tan, T. E. Eastman, J. D. Craven, and L. A. Frank (1996), Evidence of high-latitude reconnection during northward IMF: Hawkeye observations, *Geophys. Res. Lett.*, **23**, 583.
- King, J. H., and N. E. Papitashvili (2005), Solar wind spatial scales in and comparisons of hourly Wind and ACE plasma and magnetic field data, *J. Geophys. Res.*, **110**, A02209, doi:10.1029/2004JA010804.
- Kullen, A. (2000), The connection between transpolar arcs and magnetotail rotation, *Geophys. Res. Lett.*, **27**, 73.
- Kullen, A., and P. Janhunen (2004), Relation of polar auroral arcs to magnetotail twisting and IMF rotation: A systematic MHD simulation study, *Ann. Geophys.*, **22**, 951.
- Kullen, A., and T. Karlsson (2004), On the relation between solar wind, pseudobreakups, and substorms, *J. Geophys. Res.*, **109**, A12218, doi:10.1029/2004JA010488.
- Kullen, A., M. Brittnacher, J. A. Cumnock, and L. G. Blomberg (2002), Solar wind dependence of the occurrence and motion of polar auroral arcs: A statistical study, *J. Geophys. Res.*, **107**(A11), 1362, doi:10.1029/2002JA009245.
- Lepping, R. P., J. A. Jones, and L. F. Burlaga (1990), Magnetic field structure of interplanetary magnetic clouds at 1 AU, *J. Geophys. Res.*, **95**, 11,957.
- Liou, K., P. T. Newell, and C.-I. Meng (1998), Characteristics of the solar wind controlled auroral emissions, *J. Geophys. Res.*, **103**, 17,543.
- Liou, K., P. T. Newell, and C.-I. Meng (2001), Seasonal effects on auroral particle acceleration and precipitation, *J. Geophys. Res.*, **106**, 5531.
- Liou, K., C.-C. Wu, R. P. Lepping, P. T. Newell, and C.-I. Meng (2002), Midday sub-auroral patches (MSPs) associated with interplanetary shocks, *Geophys. Res. Lett.*, **29**(16), 1771, doi:10.1029/2001GL014182.
- Liou, K., J. M. Ruohoniemi, P. T. Newell, R. Greenwald, C.-I. Meng, and M. R. Hairston (2005), Observations of ionospheric plasma flows within theta auroras, *J. Geophys. Res.*, **110**, A03303, doi:10.1029/2004JA010735.
- Makita, K., and C.-I. Meng (1989), Occurrence conditions for two different kinds of transpolar arc, in *Proc. NIRP Sympos. Upper Atmos. Phys.*, vol. 2, 123 pp.
- Naehr, S. M., and F. R. Toffoletto (2004), Quantitative modeling of the magnetic field configuration associated with the theta aurora, *J. Geophys. Res.*, **109**, A07202, doi:10.1029/2003JA010191.

- Newell, P. T., and C.-I. Meng (1985), Creation of theta-auroras - The isolation of plasma sheet fragments in the polar-cap, *Science*, 270(5240), 1338.
- Newell, P. T., C.-I. Meng, and K. M. Lyons (1996), Suppression of discrete aurorae by sunlight, *Nature*, 381, 766.
- Obara, T., M. Kitayama, T. Mukai, N. Kaya, J. S. Murphree, and L. L. Cogger (1988), Simultaneous observations of sun-aligned polar cap arcs in both hemispheres by EXOS-C and Viking, *Geophys. Res. Lett.*, 15, 713.
- Ohtani, S., G. Ueno, and T. Higuchi (2005), Annual and semiannual variations of the location and intensity of large-scale field-aligned currents, *J. Geophys. Res.*, 110, A01216, doi:10.1029/2004JA010634.
- Ostgaard, N., S. B. Mende, H. U. Frey, L. A. Frank, and J. B. Sigwarth (2003), Observations of non-conjugate theta aurora, *Geophys. Res. Lett.*, 30(21), 2125, doi:10.1029/2003GL017914.
- Shue, J.-H., P. T. Newell, K. Liou, and C.-I. Meng (2001a), The quantitative relationship between auroral brightness and solar EUV Pedersen conductance, *J. Geophys. Res.*, 106, 5883.
- Shue, J.-H., P. T. Newell, K. Liou, and C.-I. Meng (2001b), Influence of interplanetary magnetic field on global auroral patterns, *J. Geophys. Res.*, 106, 5913.
- Shue, J.-H., P. T. Newell, K. Liou, and C.-I. Meng (2002), Solar wind density and velocity control of auroral brightness under normal interplanetary magnetic field conditions, *J. Geophys. Res.*, 107(A12), 1428, doi:10.1029/2001JA009138.
- Slinker, S. P., J. A. Fedder, D. J. McEwen, Y. Zhang, and J. G. Lyon (2001), Polar cap study during northward interplanetary magnetic field on 19 January 1998, *Phys. Plasmas*, 8, 1119.
- Torr, M. R., et al. (1995), A far ultraviolet imager for the international solar-terrestrial physics mission, *Space Sci. Rev.*, 71, 329.
- Tsurutani, B. T., and W. D. Gonzalez (1997), The interplanetary causes of magnetic storms: A review, in *Magnetic Storms, Geophys. Monogr., Ser.*, vol. 98, edited by B. T. Tsurutani et al., AGU, Washington, D. C.
- Valladares, C. E., H. C. Carlson Jr., and K. Fukui (1994), Interplanetary magnetic field dependency of stable sun-aligned polar cap arcs, *J. Geophys. Res.*, 99, 6247.
- Zhou, X., and B. T. Tsurutani (1999), Rapid intensification and propagation of the dayside aurora: Large scale interplanetary pressure pulses (fast shocks), *Geophys. Res. Lett.*, 26, 1097.

J. A. Cumnock, Center for Space Sciences, University of Texas at Dallas, Richardson, TX 75083, USA. (cumnock@utdallas.edu)

T. Karlsson, Space and Plasma Physics, School of Electrical Engineering, Royal Institute of Technology, SE-10044 Stockholm, Sweden. (tkarlsson@alfvenlab.kth.se)

A. Kullen, Swedish Institute of Space Physics, Uppsala Division, SE-75121 Uppsala, Sweden. (kullen@irfu.se)